

This article was downloaded by: [Moskow State Univ Bibliote]

On: 15 April 2012, At: 12:57

Publisher: Taylor & Francis

Informa Ltd Registered in England and Wales Registered Number: 1072954 Registered office: Mortimer House, 37-41 Mortimer Street, London W1T 3JH, UK



Molecular Crystals and Liquid Crystals

Publication details, including instructions for authors and subscription information:

<http://www.tandfonline.com/loi/gmcl20>

Synthesis and Characterization of Novel Chiral Liquid Crystalline Monomers and Polymers Derived From Menthol

Xiao-Xu Xu^a

^a College of Chemical Engineering and Material, Eastern Liaoning University, Dandong, People's Republic of China

Available online: 20 Mar 2012

To cite this article: Xiao-Xu Xu (2012): Synthesis and Characterization of Novel Chiral Liquid Crystalline Monomers and Polymers Derived From Menthol, *Molecular Crystals and Liquid Crystals*, 557:1, 118-125

To link to this article: <http://dx.doi.org/10.1080/15421406.2011.637390>

PLEASE SCROLL DOWN FOR ARTICLE

Full terms and conditions of use: <http://www.tandfonline.com/page/terms-and-conditions>

This article may be used for research, teaching, and private study purposes. Any substantial or systematic reproduction, redistribution, reselling, loan, sub-licensing, systematic supply, or distribution in any form to anyone is expressly forbidden.

The publisher does not give any warranty express or implied or make any representation that the contents will be complete or accurate or up to date. The accuracy of any instructions, formulae, and drug doses should be independently verified with primary sources. The publisher shall not be liable for any loss, actions, claims, proceedings, demand, or costs or damages whatsoever or howsoever caused arising directly or indirectly in connection with or arising out of the use of this material.

Synthesis and Characterization of Novel Chiral Liquid Crystalline Monomers and Polymers Derived From Menthol

XIAO-XU XU*

College of Chemical Engineering and Material, Eastern Liaoning University,
Dandong, People's Republic of China

The synthesis of two chiral mesogenic monomers (IM–IIM) derived from menthol and the corresponding polymers (IP–IIP) is described in this study. The chemical structures were characterized by FT-IR and ^1H NMR spectra. The thermal properties and optical textures were investigated by differential scanning calorimetry (DSC), thermogravimetric analysis (TGA), and polarizing optical microscopy (POM). IM and IIM showed cholesteric phase and blue phase. IM also exhibited a chiral smectic C phase. IP and IIP showed a smectic A (SmA) phase, this indicated that the liquid crystalline (LC) polymers with siloxane chains tended to form a lower order smectic phase. TGA reveals that the temperatures at which 5% mass loss occurred of the polymers obtained were above 310°C.

Keywords Chiral; liquid crystalline polymers; menthol; monomers

1. Introduction

In recent years, chiral liquid crystalline (LC) materials have attracted considerable interest, because of their unique optical-electric properties, including the selective reflection of light, thermochromism and ferroelectricity, and potential applications such as nonlinear optical devices, fast switching and full-color thermal imaging, etc. [1–12]. In general, LC compounds with rod-like and chiral molecules show a cholesteric phase and a chiral smectic C (SmC*) phase. Recently, many investigations on the synthesis and characterization of chiral LC materials, based on cholesterol, (S)-(+)-2-methyl-1-butanol, etc., have been reported, and work continues in extending the range of these materials and exploring their application [13–21]. Today, to the best of our knowledge, synthesis and characterization on the LC monomers derived from menthol and their polymers are not reported, although menthol derivatives have been used as a nonmesogenic chiral monomer for the synthesis of side chain chiral LC polymers [22–29]. Therefore, it would be both necessary and useful to synthesize LC compounds based on menthol to study structure–property relationships and explore their potential applications.

In this study, two new chiral LC monomers derived from menthol and the corresponding polymers were prepared and characterized. Their thermal properties and optical texture were

*Address correspondence to Xiao-Xu Xu, College of Chemical Engineering and Material, Eastern Liaoning University, Dandong, 118004, People's Republic of China. E-mail: 3x.931@163.com

investigated with differential scanning calorimetry (DSC), polarizing optical microscopy (POM), and thermogravimetric analysis (TGA).

2. Experimental

2.1. Materials

Allyl bromide was purchased from Beijing Chemical Reagent Co. Undecylenic acid was purchased from Beijing Jinlong Chemical Reagent Co., Ltd. 4-Hydroxybenzoic acid was obtained from Shanghai Wulian Chemical Plant. 4,4'-Dihydroxybiphenyl (from Aldrich) was used as received. L-Menthol was purchased from Shanghai Kabo Chemical Co. Chloroacetic acid was purchased from Tianjin Bodi Chemical Co. Polymethylhydrosiloxane (PMHS) was purchased from Jilin Chemical Industry Co. All solvents and reagents used were purified by standard methods.

2.2. Measurements

FT-IR spectra were measured on a Perkin-Elmer spectrum One (B) spectrometer. ^1H NMR spectra were obtained with a Bruker ARX300 spectrometer. The thermal properties were determined with a Netzsch DSC 204 equipped with a cooling system. The heating and cooling rates were $20^\circ\text{C}/\text{min}$. A Leica DMRX POM equipped with a Linkam THMSE-600 cool and hot stage was used to observe optical textures. The thermal stability of the polymers under nitrogen atmosphere was measured with a Netzsch TGA 209C thermogravimetric analyzer. The heating rates were $20^\circ\text{C}/\text{min}$.

2.3. Synthesis of the Compounds

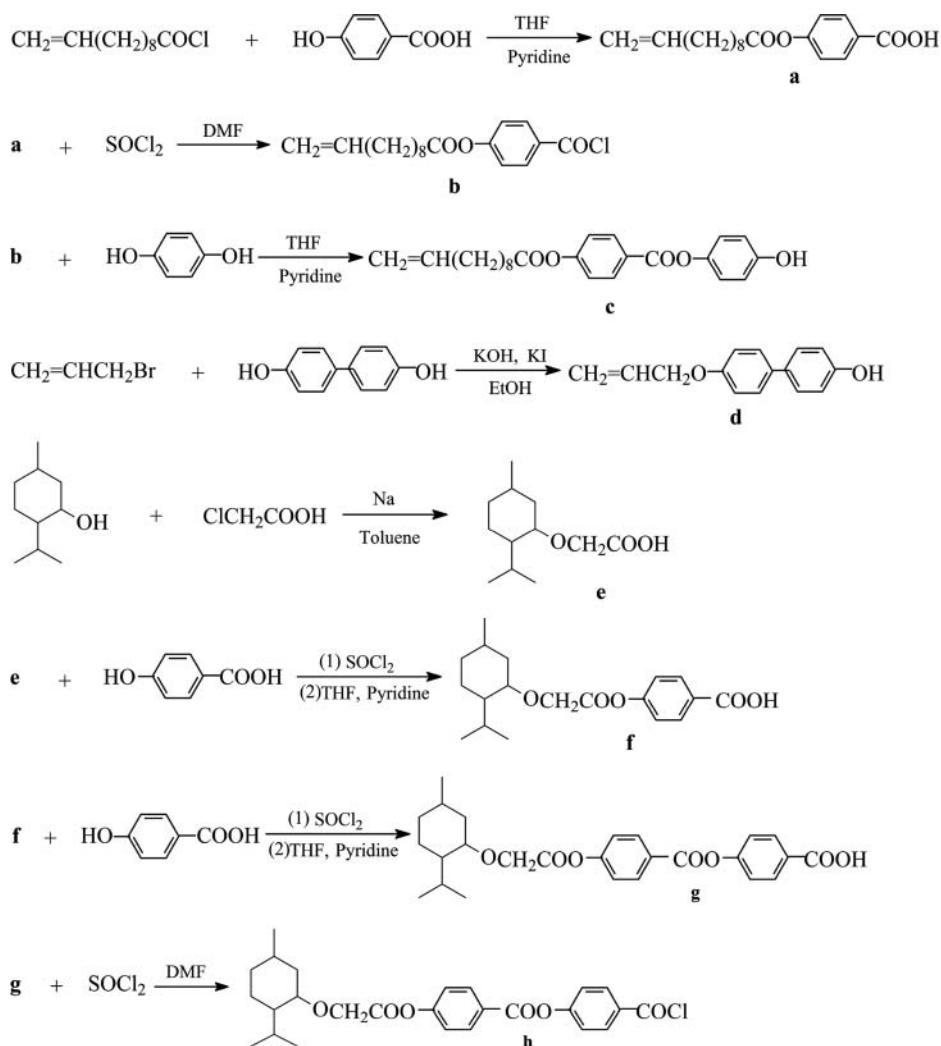
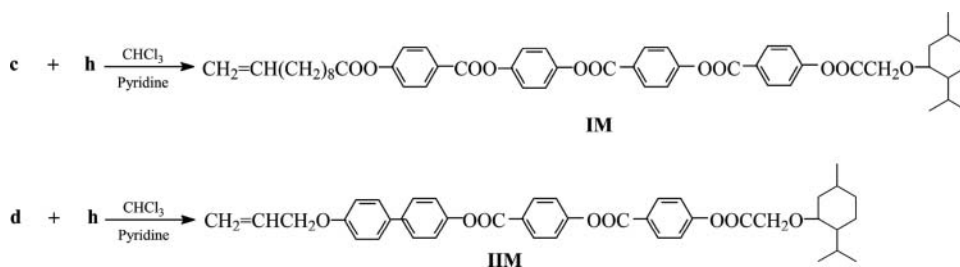
The synthetic route of the compounds **a–f** is outlined in Scheme 1. 4-(Undec-10-enoyloxy) benzoic acid (**a**), 4-hydroxyphenyl-4'-(undec-10-enoyloxy)benzoate (**c**), 4-allyloxy-4'-hydroxybiphenyl (**d**), and 4-menthyloxyacetoxybenzoic acid (**f**) were prepared according to the method reported previously [21,30].

2.3.1. 4-(4'-Menthyloxyacetoxybenzoyloxy)benzoic Acid (g). 4-Menthyloxyacetoxybenzoyl chloride was prepared through the reaction of compound **f** with excess thionyl chloride. The compound **f** (6.68 g, 0.02 mol), dissolved in 25 ml of tetrahydrofuran (THF), was added dropwise to a solution of 4-hydroxybenzoic acid (3.45 g, 0.025 mol) in 30 ml of THF and 1.6 ml of pyridine. The mixture was reacted for 2 h at room temperature, and then refluxed for 24 h. After removing the solvent by rotatory evaporate, the residue was poured into a beaker filled with 200 ml of ice water. The crude product, obtained by filtration, was washed several times with water, and then recrystallized from ethanol. A solid **g** was obtained (yield 72%, m.p. 131°C).

IR (KBr, cm^{-1}): 3076 ($=\text{C}-\text{H}$); 2950, 2845 ($-\text{CH}_2-$); 1646 ($\text{C}=\text{C}$); 1608, 1505 ($\text{Ar}-$); 1256 ($\text{C}-\text{O}-\text{C}$).

2.4. Synthesis of the Monomers

The synthetic route of the chiral olefinic monomers **IM–IIM** is shown in Scheme 2. Their synthesis is presented by the same method.

Scheme 1. Synthetic route of the intermediate compounds **a**–**h**.Scheme 2. Synthetic route of the chiral monomers **IM** and **IIM**.

2.4.1. 4-(4-(Undec-10-enyloxy)benzoyloxy)phenyl-4'-(4-(menthyloxyacetoxy)-benzoyloxy)benzoate (IM). The compound **g** (4.54 g, 0.01 mol) was dissolved in 10 ml of chloroform, and then added dropwise to a solution containing the compound **c** (4.7 g, 0.01 mol) in 25 ml of chloroform and 0.8 ml of pyridine. The reaction mixture was refluxed for 36 h, and then concentrated. The crude product was precipitated by adding methanol to the filtrate, and recrystallized from ethanol. Yield: 66%. mp: 95°C. IR (KBr, cm^{-1}): 3076 ($=\text{C}-\text{H}$); 2925, 2853 ($-\text{CH}_2-$); 1785, 1756 ($\text{C}=\text{O}$); 1640 ($\text{C}=\text{C}$); 1602, 1458 ($\text{Ar}-$); 1201 ($\text{C}-\text{O}-\text{C}$). ^1H NMR (CDCl_3 , TMS, δ): 0.85–2.64 [m, 34H, $-(\text{CH}_2)_8-$ and in menthyl-**H**]; 3.27–3.35 (m, 1H, $-\text{CH}<$ in menthyl); 4.37–4.50 (m, 2H, $-\text{OOCCH}_2\text{O}-$); 4.94–5.03 (m, 2H, $\text{CH}_2=$); 5.79–5.90 (m, 1H, $=\text{CH}-$); 7.17–8.35 (m, 16H, $\text{Ar}-\text{H}$).

2.4.2. 4-(p-Allyloxybiphenyl)-4'-(4-(menthyloxyacetoxy)benzoyloxy)benzoate (IIM). The monomer **IIM** was synthesized by reacting the compound **g** with in chloroform and pyridine. The crude product obtained was recrystallized from ethanol/acetone (2:1). Yield: 66%. mp: 95°C. IR (KBr, cm^{-1}): 3077 ($=\text{C}-\text{H}$); 2953, 2867 ($-\text{CH}_2-$); 1778, 1732 ($\text{C}=\text{O}$); 1646 ($\text{C}=\text{C}$); 1601, 1456 ($\text{Ar}-$); 1169 ($\text{C}-\text{O}-\text{C}$). ^1H NMR (CDCl_3 , TMS, δ): 0.87–1.83 [m, 18H, in menthyl-**H**]; 3.25–3.31 (m, 1H, $-\text{CH}<$ in menthyl); 4.35–4.63 (m, 4H, $-\text{OOCCH}_2\text{O}-$) and $-\text{CH}_2\text{O}-$; 5.31–5.51 (m, 2H, $\text{CH}_2=$); 6.02–6.10 (m, 1H, $\text{CH}_2=\text{CH}-$); 7.15–8.32 (m, 16H, $\text{Ar}-\text{H}$).

2.5. Synthesis of the Polymers

The polymers **IP** and **IIP** were prepared through a hydrosilylation reaction using an excess amount of olefinic monomers (5 mol% excess versus the Si-H groups in PMHS) and PMHS in toluene. The reaction mixture was heated to 60°C in the presence of H_2PtCl_6 catalyst. The reaction was held for 36 h. The polymer was obtained by precipitation from toluene solution into methanol, purified by several filtrations from hot ethanol, and then dried in a vacuum.

3. Results and Discussion

3.1. Optical Textures

In general, the rod-like, chiral molecules responsible for the macroscopical alignment of the mesogenic domains can produce cholesteric, blue, or chiral SmC^* phases. The SmC^* phase usually exhibits a broken fan-shaped texture, while the cholesteric phase exhibits an oily streak texture and a focal conic texture.

The optical textures of **IM** and **IIM** were studied by POM with a heating stage. **IM** exhibited a broken fan-shaped texture of the SmC^* phase and an oily streak texture of the cholesteric phase on heating, and a platelet texture of a cubic blue phase (BP), a focal conic texture of the cholesteric phase, and a broken fan-shaped texture of the SmC^* phase on cooling. **IIM** only showed a cholesteric phase, and exhibited an oily streak texture, a platelet texture, and a focal conic texture on the heating and cooling cycles. The optical textures of **IM**, as examples, are shown in Fig. 1. In addition, the BP is a frustrated defect phase, generally observed in a temperature interval smaller than 1°C, between the isotropic phase and the cholesteric phase of highly chiral mesogens. The BP exhibited a different color corresponding to different lattice planes, which shows Bragg scattering at different wavelengths, because the condition for constructive interference depends on the distance

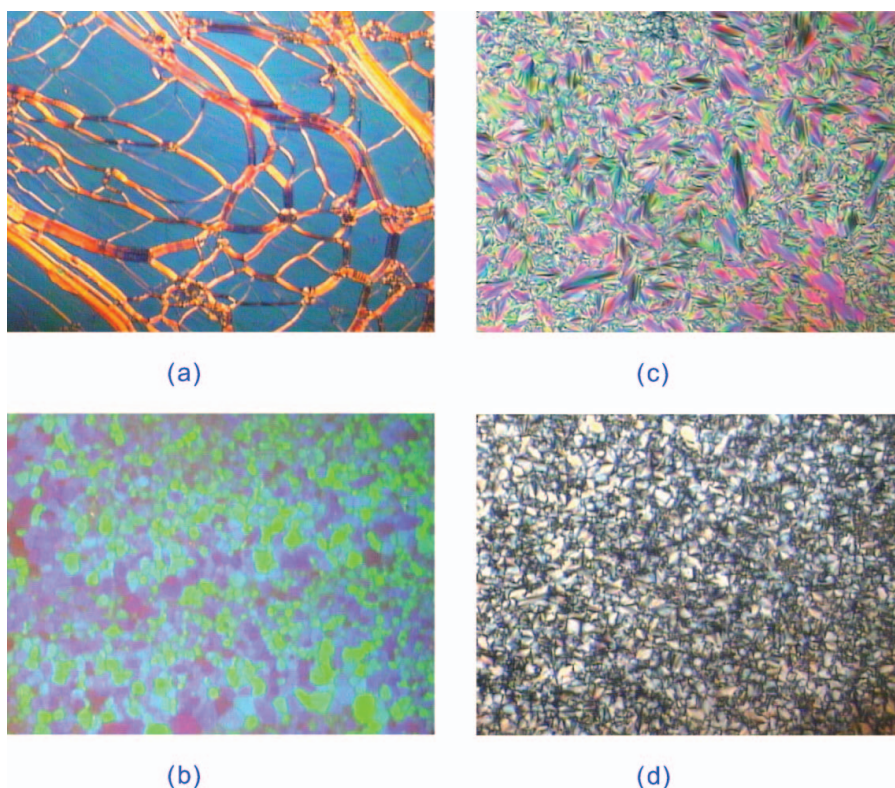


Figure 1. Optical textures of **IM** (200 \times). (a) oily streak texture of cholesteric phase on heating to 131°C; (b) platelet texture of a cubic blue phase on cooling to 171°C; (c) focal conic texture of cholesteric phase on cooling to 167°C; (d) broken fan-shaped texture of SmC* phase on cooling to 105°C.

between the lattice planes and their orientation with respect to the direction of the incident light [31].

The unique optical properties of the SmC* and the cholesteric LC materials are related to their helical supermolecular structure. The periodic helical structure selectively reflects visible light like an ordinary diffraction grating. It is known that the reflection wavelength depends on the pitch, and the pitch depends on the molecular structure and external conditions. The reflection color mainly exhibited red in the SmC* phase and blue in the cholesteric phase for **IM**, and green in the cholesteric phase for **IIM**. In addition, $dP/dT > 0$ for SmC* phase, and $dP/dT < 0$ for cholesteric phase, so the reflection wavelength or reflection color is temperature dependent. Therefore, the selective reflection shifted to the long wavelength region (red shift) in the SmC* phase and to the short wavelength region (blue shift) in the cholesteric phase with increasing temperature.

POM showed that **IP–IIP** exhibited a needle batonnet texture of a smectic A (SmA) phase, although their corresponding monomers showed SmC* and cholesteric phases. This indicates that the polymer chains hinder the formation of the helical supermolecular structure of the mesogenic units. Moreover, the LC polymers with siloxane macromolecular chains tend to form lower order smectic phases.

Table 1. Phase transition temperature ($^{\circ}\text{C}$) and enthalpy changes ($\text{J}\cdot\text{g}^{-1}$) of monomers

Monomers	$[\alpha]_D^{25\text{a}}$	Mesophase and phase transitions/heating/cooling	
IM	−24.5	K95.5(7.3)S _C *115.1(0.8) Ch172.5(0.4)I	I168.5(0.4)Ch108.5 (4.3)S _C *84.7(9.1)K
IIM	−36.1	K114.5(29.1)Ch209.6(1.0)I	I174.5(1.1)Ch98.7 (1.1)K

Note: K, crystal, S_C*, chiral smectic C phase; Ch, cholesteric phase; I, isotropic.

^aSpecific optical rotation, about 0.19 g in 100 ml of CHCl₃.

3.2. Thermal Properties

The thermal properties of the monomers and polymers were investigated with DSC, POM, and TGA. The phase transition temperatures, corresponding enthalpy changes, and mesophase types of **IM**–**IIM** and **IP**–**IIP** are summarized in Tables 1 and 2. All phase transitions are reversible, and the transition temperatures noted with DSC are consistent with those observed by POM.

DSC heating curves of **IM** showed a melting transition at 95.5 $^{\circ}\text{C}$, a SmC* to cholesteric phase transition at 115.1 $^{\circ}\text{C}$, and a cholesteric to isotropic phase transition at 172.5 $^{\circ}\text{C}$, respectively. On cooling, three exothermic peaks were seen, which represent an isotropic to cholesteric phase transition at 168.5 $^{\circ}\text{C}$, a cholesteric to SmC* phase transition at 108.5 $^{\circ}\text{C}$, and a SmC* to crystallization transition at 84.7 $^{\circ}\text{C}$, respectively. **IIM** showed a melting transition at 114.5 $^{\circ}\text{C}$ and a cholesteric to isotropic phase transition at 209.6 $^{\circ}\text{C}$ on heating process, and an isotropic to cholesteric phase transition at 174.5 $^{\circ}\text{C}$, a cholesteric to crystallization transition at 98.7 $^{\circ}\text{C}$ on cooling process.

For **IP**–**IIP**, their DSC curves all showed a glass transition at low temperature, and an LC to isotropic phase transition temperature at high temperature. Moreover, the mesophase temperature ranges of **IP**–**IIP** were greater than those of the corresponding monomers. This indicates that the polymerization effect can stabilize and widen the mesophase temperature range.

In general, with increasing the flexible spacer length, the intermolecular forces weaken, this will make the corresponding phase transition temperatures decrease. For example, compared with **IIM** containing terminal allyl spacer, T_m and T_i of **IM** containing terminal undecylenyl spacer decreased by 19.0 $^{\circ}\text{C}$ and 37.1 $^{\circ}\text{C}$, respectively. Similarly, the glass transition temperature (T_g) decreased from 32.3 $^{\circ}\text{C}$ for **IIP** to 12.8 $^{\circ}\text{C}$ for **IP**, and T_i decreased from 193.8 $^{\circ}\text{C}$ to 178.7 $^{\circ}\text{C}$.

Table 2. The phase transition temperatures and decomposition temperatures of polymers

Polymers	T_g ($^{\circ}\text{C}$)	T_i ($^{\circ}\text{C}$)	ΔH_i ($\text{J}\cdot\text{g}^{-1}$)	ΔT^a	T_d^b ($^{\circ}\text{C}$)
IP	12.8	178.7	0.8	165.9	335
IIP	32.3	193.8	2.6	161.5	315

^aMesophase temperature range ($T_i - T_g$).

^bTemperature at which 5% weight loss occurred.

The thermal stabilities of **IP**–**IIP** were detected with TGA. The corresponding data are shown in Table 2. TGA results showed that the temperatures at which 5% weight loss occurred (T_d) were greater than 310°C, this indicates that they have a good thermal stability.

4. Conclusions

Two new chiral mesogenic monomers containing menthyl groups and their corresponding polymers were synthesized and characterized. The monomers **IM** and **IM** all showed an enantiotropic cholesteric oily streak texture and a focal conic texture, as well as a platelet texture. In addition, **IM** also exhibited a broken fan-shaped texture of a SmC* phase on heating and cooling cycles. **IP** and **IP** exhibited the batonnet textures of SmA phase. With increasing the length of flexible spacer, the corresponding T_m or T_g and T_i decreased. Moreover, a flexible polysiloxane backbone, a rigid mesogenic core, and a long flexible spacer tended to generate a low glass transition temperature, a wide mesophase temperature range, and a high thermal stability.

Acknowledgment

The authors are grateful to the Educational Development of Liaoning Province for financial support of this work.

References

- [1] Broer, D. J., Lub, J., & Mol, G. N. (1995). *Nature*, 378, 467.
- [2] Day, G. M., Kim, H. J., Jackson, W. R., & Simon, G. P. (1999). *Acta. Polym.*, 50, 96.
- [3] Zheng, S. J., Li, Z. F., Zhang, S. Y., Cao, S. K., Guo, K., & Zhou, Q. F. (2000). *Polym. Advan. Technol.*, 11, 219.
- [4] Shibaev, V., Bobrovsky, A., Boiko, N., & Schaumburg, K. (2000). *Polym. Int.*, 49, 931.
- [5] Shibaev, P. V., Kopp, V. I., & Genack, A. Z. (2003). *J. Phys. Chem. B.*, 107, 6961.
- [6] Lin, Q., Pasatta, J., & Long, T. E. (2003). *J. Polym. Sci. Part A: Polym. Chem.*, 41, 2512.
- [7] Kaspar, M., Bubnov, A., Hamplova, V., Novotna, V., Lhotakova, I., Havlicek, J., & Ilavsky, M. (2005). *Mol. Cryst. Liq. Cryst.*, 448, 49.
- [8] Boiko, N. I., Lysachkov, A. I., Ponomarenko, S. A., Shibaev, V. P., & Richardson, R. M. (2005). *Colloid Polym. Sci.*, 283, 115.
- [9] Muge Calik Sahin, Y., Ersin Serhatli, I., & Menciloglu, Y. Z. (2006). *J. Appl. Polym. Sci.*, 102, 1915.
- [10] Hsiue, G. H., & Lee, R. H. (2006). *J. Polym. Sci. Part B: Polym. Phys.*, 44, 2035.
- [11] Ohta, R., Togashi, F., & Goto, H. (2007). *Macromolecules*, 40, 5228.
- [12] Suda, K., & Akagi, K. (2008). *J. Polym. Sci. Part A: Polym. Chem.*, 46, 3591.
- [13] Pfeuffer, T., & Strohmriegl, P. (1999). *Macromol. Chem. Phys.*, 200, 2480.
- [14] Zhang, B., Hu, J., Yao, D., & Zhang, L. (2003). *Acta Polym. Sin.*, 6, 799.
- [15] Hsiue, G. H., & Chen, J. H. (1995). *Macromolecules*, 28, 4366.
- [16] Hsu, C. S., Chu, P. H., Chang, H. L., & Hsieh, T. H. (1997). *J. Polym. Sci. Part A: Polym. Chem.*, 35, 2793.
- [17] Mihara, T., Nomura, K., Funaki, K., & Koide, N. (1997). *Polym. J.*, 29, 303.
- [18] Hu, J. S., Zhang, B. Y., Zhou, A. J., Du, B. G., & Yang, L. Q. (2006). *J. Appl. Polym. Sci.*, 100, 4234.
- [19] Soltysiak, J. T., Czuprynski, K., & Drzewinski, W. (2006). *Polym. Int.*, 55, 273.
- [20] Zheng, Z., Sun, Y. Y., Xu, J., Chen, B., Su, Z. Q., & Zhang, Q. J. (2007). *Polym. Int.*, 56, 699.
- [21] Zhang, B. Y., Hu, J. S., Yang, L. Q., He, X. Z., & Liu, C. (2007). *Euro. Polym. J.*, 43, 2017.
- [22] Mihara, T., Nomura, K., & Funaki, K. (1997). *Polym. J.*, 29, 309.

- [23] Bobrovsky, A. Y., Boiko, N. I., & Shibaev, V. P. (1998). *Liq. Cryst.*, *24*, 489.
- [24] Bobrovsky, A. Y., & Shibaev, V. P. (2002). *Adv. Funct. Mater.*, *12*, 367.
- [25] Lee, Y. K., Onimura, K., Tsutsumi, H., & Oishi, T. (2000). *J. Polym. Sci: Part A: Polym. Chem.*, *38*, 4315.
- [26] Hu, J. S., Zhang, B. Y., Pan, W., & Zhou, A. J. (2005). *Liq. Cryst.*, *32*, 441.
- [27] Du, B. G., Hu, J. S., Zhang, B. Y., Xiao, L. J., & Wei, K. Q. (2006). *J. Appl. Polym. Sci.*, *102*, 5559.
- [28] Liu, J. H., Yang, P. C., & Hung, H. J. (2007). *Liq. Cryst.*, *34*, 891.
- [29] Liu, J. H., Hung, H. J., Yang, P. C., & Tien, K. H. (2008). *J. Polym. Sci: Part A: Polym. Chem.*, *46*, 6214.
- [30] Hu, J. S., Wei, K. Q., Zhang, B. Y., & Yang, L. Q. (2008). *Liq. Cryst.*, *35*, 925.
- [31] Dierking, I. (2003). *Textures of liquid crystals*. Wiley-Vch Verlag GmbH & Co. KGaA: Weinheim.